Taylor & Francis
Taylor & Francis Group

REPORT

⊘ OPEN ACCESS   Ⓜ Check for updates

Site-specific conjugation allows modulation of click reaction stoichiometry for pretargeted SPECT imaging

Danielle Mandikian[a]*, Hanine Rafidi[a]*, Pragya Adhikari[b], Priya Venkatraman ⓘ[a], Lidia Nazarova ⓘ[a], Gabriel Fung ⓘ[a], Isabel Figueroa ⓘ[a], Gregory Z. Ferl[a], Sheila Ulufatu[c], Jason Ho[c], Cynthia McCaughey ⓘ[c], Jeffrey Lau[d], Shang-Fan Yu[d], Saileta Prabhu[a], Jack Sadowsky[b], and C. Andrew Boswell ⓘ[a]

[a]Preclinical and Translational Pharmacokinetics, Genentech Inc., South San Francisco, CA, USA; [b]Protein Chemistry, Genentech Inc., South San Francisco, CA, USA; [c]In Vivo Studies, Genentech Research and Early Development, South San Francisco, CA, USA; [d]Translational Oncology, Genentech Inc., South San Francisco, CA, USA

ABSTRACT

Antibody pretargeting is a promising strategy for improving molecular imaging, wherein the separation in time of antibody targeting and radiolabeling can lead to rapid attainment of high contrast, potentially increased sensitivity, and reduced patient radiation exposure. The inverse electron demand Diels-Alder 'click' reaction between trans-cyclooctene (TCO) conjugated antibodies and radiolabeled tetrazines presents an ideal platform for pretargeted imaging due to rapid reaction kinetics, bioorthogonality, and potential for optimization of both slow and fast clearing components. Herein, we evaluated a series of anti-human epidermal growth factor receptor 2 (HER2) pretargeting antibodies containing distinct molar ratios of site-specifically incorporated TCO. The effect of stoichiometry on tissue distribution was assessed for pretargeting TCO-modified antibodies (monitored by ^{125}I) and subsequent accumulation of an ^{111}In-labeled tetrazine in a therapeutically relevant HER2+tumor-bearing mouse model. Single photon emission computed tomography (SPECT) imaging was also employed to assess tumor imaging at various TCO-to-monoclonal antibody (mAb) ratios. Increasing TCO-to-mAb molar ratios correlated with increased in vivo click reaction efficiency evident by increased tumor distribution and systemic exposure of ^{111}In-labeled tetrazines. The pharmacokinetics of TCO-modified antibodies did not vary with stoichiometry. Pretargeted SPECT imaging of HER2-expressing tumors using ^{111}In-labeled tetrazine demonstrated robust click reaction with circulating antibody at ~2 hours and good tumor delineation for both the 2 and 6 TCO-to-mAb ratio variants at 24 hours, consistent with a limited cell-surface pool of pretargeted antibody and benefit from further distribution and internalization. To our knowledge, this represents the first reported systematic analysis of how pretargeted imaging is affected solely by variation in click reaction stoichiometry through site-specific conjugation chemistry.

Introduction

The exquisite target specificity of antibodies has encouraged the development of immune-imaging agents for detection and staging of cancer. However, conventional antibody-based positron emission tomographic (PET) or single photon emission computed tomography (SPECT) imaging requires the covalent attachment of radionuclides with long decay half-lives (e.g., ^{124}I, $t_{1/2}$ = 4.2 days; ^{89}Zr, $t_{1/2}$ = 3.3 days or ^{111}In, $t_{1/2}$ = 2.8 days) to match the long circulation half-lives of antibodies (prolonged by endothelial recycling mediated by the neonatal Fc receptor, FcRn)[1] and time required for their target distribution.[2] The slow distribution phase also makes it difficult to perform convenient same-day imaging, limits the number of scans due to high patient radiation doses, and has prompted the search for alternative pre-targeted approaches.

Pretargeting is a two-step process in which a targeting agent is administered and allowed sufficient time to specifically localize and bind to a target, followed by administration of a second, radiolabeled molecule that binds to or reacts with the pretargeting agent to effectively achieve radiolabeling in vivo.[3] In antibody pretargeting, the molecular uncoupling of the slowly clearing, targeting antibody from the radiolabel presents an opportunity to acquire images using faster decaying radionuclides such as ^{68}Ga ($t_{1/2}$ = 68 min) and ^{18}F ($t_{1/2}$ = 110 min). Direct comparisons to directly labeled methods suggest that pretargeting methods could reduce patient radiation exposure during imaging procedures by 1–2 orders of magnitude,[4] with benefits also possible for pretargeted radioimmunotherapy.[5] Use of pretargeted imaging can decrease radiation dosimetry relative to traditional methods in multiple ways: by delaying the time of introduction of radioactivity, by reducing the whole-body retention of injected radioactive dose (which depends on stoichiometry and binding/reaction efficiency) and by allowing the use of radionuclides having shorter decay half-lives. The ability to image with faster decaying radionuclides not only limits patient radiation exposure, but also provides more

---

flexibility in radiotracer chemistry, with potential advantages in manufacturing and isotope costs. Clinical evaluations of pre-targeted imaging with bispecific antibodies,[6,7] streptavidin/biotin pretargeting,[8,9] and radiolabeled haptens[10] have yielded encouraging results.

One of the most robust reactions within the click chemistry repertoire is the inverse electron demand Diels-Alder (IEDDA) reaction between a *trans*-cyclooctene (TCO) and an *s*-tetrazine (Figure 1A).[11] These IEDDA reactions have second-order rate constants ranging from $k_2 = 10^3–10^6$ $M^{-1}s^{-1}$, which are primarily driven by expulsion of N_2 and TCO strain relief following the cycloaddition[12,13] Furthermore, electron withdrawing substituents attached to the tetrazine confer increased reaction rates between the dienophile and diene.[14,15] Successful pretargeted *in vivo* nuclear imaging has been demonstrated in preclinical models using PET isotopes, including [11]C ($t_{1/2}$ 20.3 minutes),[16,17] [18]F ($t_{1/2}$ 110 minutes)[18–20] and [64]Cu ($t_{1/2}$ 12.7 hours),[4,21–24] as well as SPECT isotopes including [99m]Tc ($t_{1/2}$ 6 hours),[25–27] [111]In ($t_{1/2}$ 2.8 days)[28–30] and [177]Lu ($t_{1/2}$ 6.7 days).[27,31–33] The recent success of IEDDA reactions for *in vivo* pretargeting and other chemical biology applications has been reviewed by several groups.[12,34–37] Most examples incorporate TCO on the slower clearing molecule followed by a fast clearing radiolabeled tetrazine tracer, but some groups have explored reversing the chemistry.[38,39]

Most pretargeting antibodies have targeted highly expressed, non-internalizing antigens such as A33, CA19.9, and tumor-associated glycoprotein 72 (TAG-72) glycoproteins.[4,23,30] While these early imaging studies were successful, highly expressed non-internalizing targets only represent a fraction of clinically relevant oncology targets since many cell-surface cancer targets are internalizing. For instance, clinical imaging of human epidermal growth factor receptor 2 (HER2)-expressing tumors has been actively pursued via directly labeled antibodies,[40,41] antibody fragments[42] and affibodies[43] in an effort to improve patient selection and response monitoring for HER2-targeted cancer therapies.[44] Fewer examples exist in which internalizing targets have been pretargeted,[20,39] likely due to risk of time-dependent cell surface depletion of TCO moieties available for click reaction through antibody-bound receptor internalization, thereby decreasing image contrast. For instance, use of enzyme-based approaches for pretargeted imaging as an alternative to IEDDA reactions was successful for a non-internalizing antigen (TAG-72), but not for an internalizing antigen (HER2).[45] However, there is a recent interest in pretargeted imaging of internalizing targets such as HER2 despite these challenges.[20,39]

The use of IEDDA reactions for PET/SPECT imaging has been largely explored using TCO-modified pretargeting antibodies. Apart from a few examples,[21] TCO conjugation methods have most commonly been through random lysine modifications, yielding a highly variable range of TCO-to-monoclonal antibody (mAb) ratios. Furthermore, the previous effort in site-specific conjugation did not allow for variation in TCO-to-mAb ratio.[21] The inability to carefully control TCO-to-mAb ratios has made it difficult to regulate *in vivo* reaction stoichiometry, thus warranting evaluation of site-specific conjugation approaches.
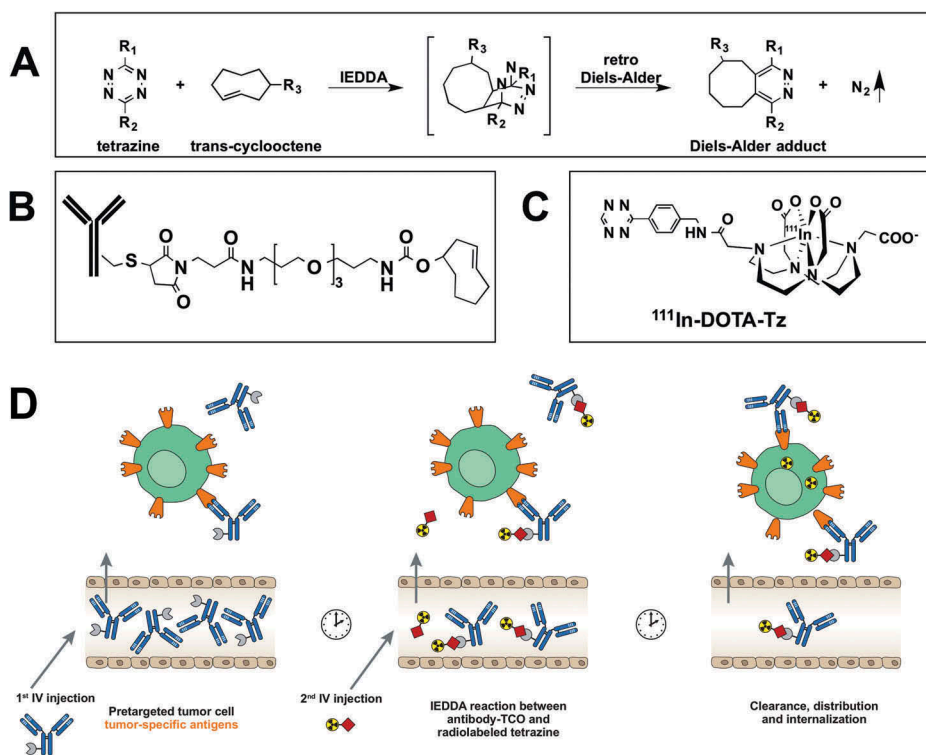

Figure 1. Click chemistry reagents and pre-targeting for imaging. **(A)** Generic inverse electron demand Diels-Alder reaction (IEDDA) between a *trans*-cyclooctene (TCO) and disubstituted 1,2,4,5-tetrazine. The robustness of the reaction is afforded by a fast *retro* Diels-Alder step to generate N_2. **(B)** THIOMAB™ antibodies are modified at engineered cysteine residues for controlled molar ratios of incorporated TCOs ranging from 2 to 6 moles of TCO per Mole of antibody. **(C)** The tetrazine used for this study, ^{111}In-DOTA-Tz. **(D)** Simplified schematic of antibody pretargeting using TCO/tetrazine click chemistry. TCO-modified antibody is allowed to distribute and accumulate at tumor of interest, followed by injection of radiolabeled tetrazine after maximal antibody distribution. Diels-Alder reaction occurs, tagging surface antibodies with radiolabel and providing tumor contrast in SPECT imaging in a time-dependent manner.

Herein, we present results from the pretargeted biodistribution and imaging of HER2-positive breast cancer xenografts in mice using TCO/tetrazine chemistry. We conjugated TCO moieties, via short polyethylene glycol (PEG) linkers, site-specifically to anti-HER2 THIOMAB™ antibodies[46] with varying numbers of engineered cysteines[47] to determine the importance of stoichiometry on the in vivo IEDDA reaction in a HER2-positive KPL-4 tumor model. We employed ^{111}In ($t_{1/2}$ 2.8 days) to allow direct comparison between our conventional radioimmunoconjugate and our click reactive tetrazine probe in an attempt to demonstrate proof of concept for same-day imaging with shorter lived radionuclides such as ^{68}Ga ($t_{1/2}$ = 68 min). To our knowledge, this is the first reported use of site-specific conjugation chemistry to systematically evaluate the effect of varying the TCO-to-mAb ratio for pretargeted imaging while maintaining consistent linker chemistry.

Results

THIOMAB™ antibody TCO conjugations

Conjugation ratios determined by liquid chromatography-mass spectrometry (LC-MS) analysis were 1.9 (LC:K149C), 3.7 (LC: K149C, HC:L177C) and 5.5 (LC:K149C, HC:L177C, HC:Y376C) for 7C2-TCO$_2$, 7C2-TCO$_4$ and 7C2-TCO$_6$, respectively. The LC-MS chromatograms are presented in **Supplemental Figure S2**. TCO-PEG$_3$-maleimide was conjugated through the engineered thiols, with ~95% efficiency (Figure 1B). DOTA-maleimide conjugation to 7C2-LC:K149C produced a molar ratio of 1.9. Table 1 summarizes the various antibody conjugates evaluated herein with mutation sites and molar ratios.

Radiochemistry

Radioiodination of 7C2, 7C2-TCO$_2$, 7C2-TCO$_4$, and 7C2-TCO$_6$ with 37 MBq input yielded ~ 65% radiochemical yields for all antibodies. Radiometal labeling of DOTA-modified antibody provided ^{111}In-DOTA$_2$-7C2 (~41 kBq/µg, 23% yield) and was sufficient for invasive tissue distribution. The low radiochemical yield (likely due to only two copies of DOTA per antibody) was not sufficient to appropriately dose animals for SPECT imaging (which requires high activity), prompting us to use ^{111}In-DOTA$_6$-7C2 (~7.8 MBq/µg, 77% yield) for imaging. Radio metal labeling of DOTA-Tz (Figure 1C) for invasive bio distribution studies provided ^{111}In-DOTA-Tz (4.3 MBq/µg, 95%

radiochemical yield). Large scale radiometal labeling of DOTA-Tz for SPECT-CT yielded sufficient ^{111}In-DOTA-Tz for imaging studies (1.5 MBq/µg based on the amount of tetrazine prior to Sep-Pak, ~34% radiochemical yield after Sep-Pak). Radiochemical purities were 98% for ^{111}In-DOTA-Tz, ranging from 96–98% for all ^{125}I-labeled 7C2 antibodies and at least 96–99% for all ^{111}In-DOTA-labeled 7C2 antibodies. Representative radiochromatograms are presented in **Supplemental Figure S3**.

In vitro click reactivity correlated with increased TCO conjugation

To demonstrate proof-of-concept for antibody pretargeting with our TCO-modified 7C2 antibodies, and to determine if increasing TCO conjugation levels improve the signal-to-noise ratio, we performed in vitro click reactions using cultured HER2-expressing KPL-4 cells. The ^{125}I signal was used to assess intact antibody bound to the surface of cells, represented as the % of antibody incubated (%AI). In contrast, the ^{111}In signal reflected surface bound or internalized tetrazine, represented as % of tetrazine incubated (%TI) (Figure 2). To encourage constant HER2 receptor occupancy despite internalization, antibody concentrations in the cell media were in far excess of the number of cell surface receptors; this resulted in small percentages of bound antibody relative to the amount incubated. The incubated ^{125}I-7C2 antibodies ranged from 2.06 to 3.46 %AI, indicating that TCO conjugation did not dramatically affect binding of antibodies to HER2 (Figure 2A). In contrast, the ^{111}In-DOTA-Tz signal significantly increased compared to the 7C2 control, proportional to the amount of TCO groups available for Diels-Alder reaction. The 7C2 control had 0.03 %TI, and the addition of 2 TCO molecules led to a significant 13-fold increase to 0.39 %TI for 7C2-TCO$_2$. Each subsequent molar addition of two TCO molecules lead to a significant 1.5-fold increase in %TI, with 0.57 %TI for 7C2-TCO$_4$ and up to 0.91 %TI for 7C2-TCO$_6$ pretargeting antibody treatment (Figure 2B).

In vivo click reactions occurred rapidly and increased systemic exposure of radiolabeled tetrazine derivatives

We performed in vivo click reaction in KPL-4 tumor-bearing mice. Mice received single intravenous (IV) injections of iodinated and TCO-modified antibodies (total antibody dose of 5 mg/kg), followed 24 hours later by tracer levels (~7- to 25-fold lower than TCO on a molar basis for ^{111}In-DOTA-Tz, see Table 2) of ^{111}In-DOTA-Tz (~0.7 kDa) (Figure 1C and **Supplemental Figure S1A**). The dose of 5 mg/kg was chosen as a balance to ensure sufficient numbers of TCO groups for click reaction, but without saturating HER2 dependent tumor uptake. Monitoring the levels of radioiodinated antibodies showed that TCO conjugation did not affect the short-term systemic exposure, represented by the area under the curve from 0 to 2 days (AUC$_{0-2}$, in units of %ID/mL•day), at 2-fold molar (AUC$_{0-2}$ 54.3 ± 2.6, p > 0.05) and 6-fold molar (AUC$_{0-2}$ 49.6 ± 2.9, p > 0.05) TCO-to-mAb ratios relative to unmodified 7C2 (AUC$_{0-2}$ 48.8 ± 3.3) (Figure 3A). Overall, antibody pharmacokinetics was consistent across all treatment groups (**Supplemental Figure S4**).

Table 1. THIOMAB™ antibody mutations and conjugation ratios.

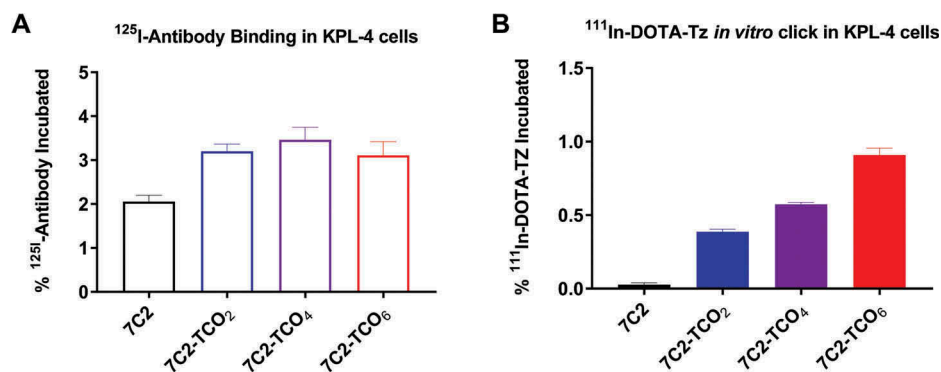| Antibody Name	Antibody Mutations	Conjugation Material	Molar Ratio DOTA	Molar Ratio TCO
7C2	LC:K149C			
7C2-DOTA$_2$	LC:K149C	DOTA-maleimide	1.9	
7C2-DOTA$_6$	LC: K149C HC: L177C HC: Y376C	DOTA-maleimide	5.9	
7C2-TCO$_2$	LC:K149C	TCO-PEG$_3$-maleimide		1.9
7C2-TCO$_4$	LC: K149C HC: L177C	TCO-PEG$_3$-maleimide		3.7
7C2-TCO$_6$	LC: K149C HC: L177C HC: Y376C	TCO-PEG$_3$-maleimide		5.5

Figure 2. ^{111}In-DOTA-Tz *in vitro* click with increasing 7C2-TCO$_x$ conjugation ratios using KPL-4 cells. KPL-4 cells were incubated with ^{125}I-labeled antibodies for 2 hours, followed by 30 min incubation with ^{111}In-DOTA-Tz. cells were harvested and subjected to gamma counting. **(A)** ^{125}I (hollow bars) and **(B)** ^{111}In (solid bars) signals represented as the % of Antibody Incubated (%AI) or % of Tetrazine Incubated (%TI) ±standard deviation. The amount of antibody incubated was intentionally in vast excess of HER2 receptor number so that internalization would not significantly deplete the antibody in the incubating solution; Hence the %AI and %TI values are low.

Table 2. Effective systemic blood concentrations[a] and TCO-to-Tetrazine ratios.

	Invasive biodistribution Figures 3 and 4 (~ 0.185 MBq ^{111}In dose)		SPECT-CT imaging Figures 5 and 6 (~ 18.5 MBq ^{111}In dose)	
Pretargeted antibody (5 mg/kg)	7C2-TCO$_2$	7C2-TCO$_6$	7C2-TCO$_2$	7C2-TCO$_6$
[TCO] (nM)	266	798	266	798
[Tz] (nM) for ^{111}In-DOTA-Tz	37	37	10,700	10,700
[TCO]/[Tz] ratio	7	22	0.025	0.075

[a] Calculated based on measured 24-hour blood concentration ([7C2-TCO$_x$]) and injected doses of ^{111}In-DOTA-Tz, assuming a 2-mL mouse blood volume

Mice receiving 7C2 (incapable of click reaction due to the absence of TCO) followed by ^{111}In-labeled tetrazines showed much lower tetrazine systemic exposure (relative to antibody exposure), measured as AUC from 1 to 2 days (AUC$_{1-2}$, in units of %ID/mL•day), with a value of 2.03 ± 0.15 for ^{111}In-DOTA-Tz (Figure 3B). In contrast, mice receiving 7C2-TCO$_x$ antibodies showed increased systemic exposure of ^{111}In-DOTA-Tz (Figure 3B) with reduced clearance compared to the 7C2 non-click reactive control group. The ^{111}In-DOTA-Tz following 7C2-TCO$_6$ pretargeting (AUC$_{1-2}$ 17.0 ± 1.5) exhibited the highest similarity in exposure to ^{125}I-7C2 (AUC$_{1-2}$ 17.5 ± 1.6, p > 0.05) (Figure 3B). Exposure of ^{111}In-DOTA-Tz (AUC$_{1-2}$) increased from 2.03 ± 0.15 to 9.45 ± 0.63 and 17.0 ± 1.5 following doses of 7C2, 7C2-TCO$_2$ and 7C2-TCO$_6$ with corresponding C$_{max}$ values (at 15 minutes; 24.25 h post 7C2) of 4.02, 11.9 and 21.9 %ID/mL, respectively. Furthermore, increasing number of TCOs per antibody by ~3-fold increased the systemic exposure of ^{111}In-DOTA-Tz by 1.8 fold (7C2-TCO$_2$ vs. 7C2-TCO$_6$, Figure 3B), similar to the trend observed with the *in vitro* binding assay (Figure 2B). Taken together, this suggests that ~40% of injected ^{111}In-DOTA-Tz (21.9 %ID/mL multiplied by a ~ 2-mL mouse total blood volume) reacted with 7C2-TCO$_6$ systemically within the first 15 min of tetrazine administration (Figure 3B).

The tetrazine probe exhibited robust in vivo click reaction in tumors

The distribution of iodinated ^{125}I-7C2, ^{125}I-7C2-TCO$_2$, and ^{125}I-7C2-TCO$_6$ antibodies revealed the overall modest
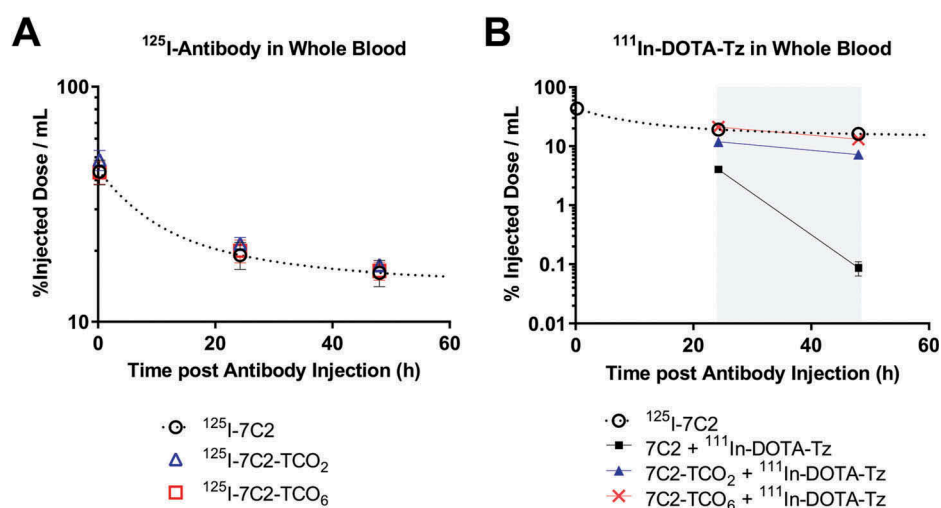

Figure 3. *In vivo* systemic exposure of 7C2, 7C2-TCO$_x$ antibodies and tetrazines. KPL-4 tumor-bearing mice received 185 kBq of ^{125}I-7C2 or ^{125}I-7C2-TCO$_x$ antibodies, followed 24 hours later with 185 kBq of ^{111}In-labeled tetrazine derivative. Whole blood was collected at 0.25, 24.25 hours (15 min post tetrazine injection) and 48 hours post antibody injection. Samples were subjected to gamma counting and values were plotted as percentage of injected dose per mL of blood. **(A)** Antibody exposure was plotted by dotted lines for 7C2 (black), 7C2-TCO$_2$ (blue) and 7C2-TCO$_6$ (red). **(B)** Since no differences in AUC$_{0-2}$ were observed among these antibodies, only the ^{125}I-7C2 curve from **A** was overlaid with the solid lines indicating tetrazine exposure for ^{111}In-DOTA-Tz.
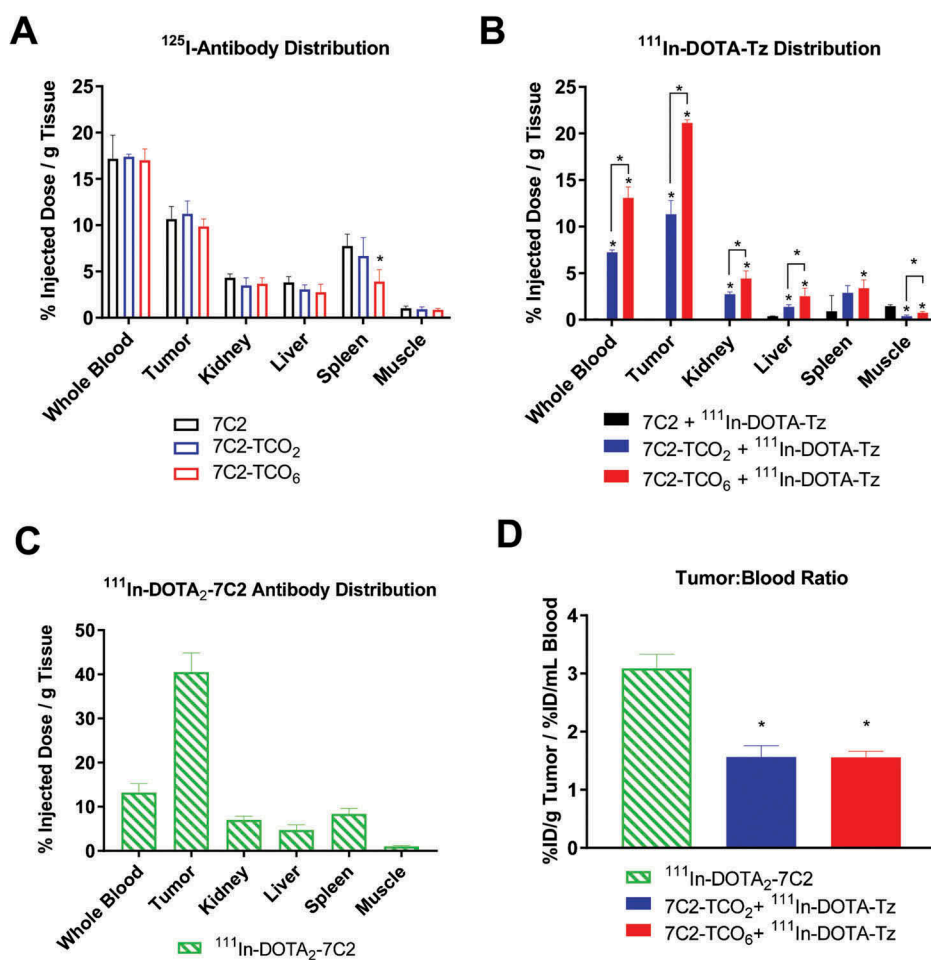
Figure 4. *In vivo* biodistribution of 7C2, 7C2-TCO$_x$ antibodies and tetrazine probe. KPL-4 tumor-bearing mice were injected with 5 mg/kg including a spike of 185 kBq of ^{125}I-7C2 or ^{125}I-7C2-TCO$_x$, followed 24 hours later by 185 kBq of ^{111}In-labeled tetrazine. directly labeled ^{111}In-DOTA$_2$-7C2 was co-injected with ^{125}I-7C2 followed by tissue harvest 48 hours later. Tissues were harvested, rinsed with PBS and weighed at 48 h post antibody injection. Samples were subjected to gamma counting and values were plotted as percentage of injected dose per gram of tissue. **(A)** Antibody distribution (hollow bars) plotted for ^{125}I-7C2 (black), ^{125}I-7C2-TCO$_2$ (blue) and ^{125}I-7C2-TCO$_6$ (red). **(B)** Tetrazine distribution (solid bars) for ^{111}In-DOTA-Tz. Data in **(A)** and **(B)** were plotted with significance compared to each respective 7C2 non-click reactive control indicated above each bar. Direct comparisons between 7C2-TCO$_2$ and 7C2-TCO$_6$ were indicated via bracket. **(C)** Antibody distribution of directly labeled ^{111}In-DOTA$_2$-7C2. **(D)** ^{111}In signal in tumor normalized to blood. Student's t-tests were performed and significance indicated by * $p < 0.05$.

effect of TCO conjugation on tumor distribution of intact (non-internalized) antibody, with respective values of 10.7, 11.2, and 8.0 %ID/g (Figure 4A). A slight trend towards reduced antibody distribution was observed for 7C2-TCO$_6$ compared to 7C2 in tumor (9.9 vs 10.7 %ID/g, p > 0.05), liver (2.6 vs 3.8 %ID/g, p > 0.05) and spleen (3.9 vs 7.8 % ID/g, p < 0.05) despite equivalent systemic exposure (Figure 4A).

The distribution of radiolabeled tetrazine following pretargeting with 7C2 and 7C2-TCO$_x$ conjugated antibodies was also compared (Figure 4B), and the impact of stoichiometry was much more striking. ^{111}In-DOTA-Tz exhibited significantly increased tumor localization, which corresponded with increased TCO conjugation ratio: 0.03 %ID/g with 7C2, 11.3 %ID/g (p < 0.05) with 7C2-TCO$_2$ and 21.1 %ID/g (p < 0.05) with 7C2-TCO$_6$ pretargeting (Figure 4B). In the same respective groups, distribution in kidney was 0.012, 2.7 and 4.4 %ID/g and in liver was 0.39, 1.4 and 2.5 %ID/g. Biodistribution data for additional tissues are available in **Supplemental Table S1**.

Tumor pretargeting produced lower tumor-to-blood ratios than direct tumor targeting

To directly compare tumor pretargeting to traditional targeting methods, selected tumor-bearing mice received ^{125}I-7C2 and ^{111}In-DOTA$_2$-7C2. The chelated radiometals are residualizing labels within both traditionally (i.e., directly) labeled ^{111}In-DOTA$_2$-7C2 and ^{111}In-DOTA-Tz. This explains the roughly 4-fold higher tumor levels of residualizing ^{111}In in Figure 4C relative to non-residualizing ^{125}I in Figure 4A. Roughly consistent with previous ^{111}In-labeled anti-HER2 antibodies,[48] ^{111}In-DOTA$_2$-7C2 exhibited tumor labeling at 40.5 %ID/g and kidney distribution at 7 %ID/g (Figure 4C). However, the traditional labeling method allowed for a total of 48 hours for the internalizing ^{111}In-DOTA$_2$-7C2 reagent to distribute, bind and accumulate, making direct comparisons difficult since ^{111}In-labeled tetrazines had only 24 hours to accumulate. Tumor-to-blood ratios for the tetrazine probe were significantly decreased with 7C2-TCO$_x$ pretargeting (~1 for both TCO$_2$ and TCO$_6$) relative to ^{111}In-DOTA$_2$-7C2 with a ratio of ~3 (Figure 4D).

Non-invasive SPECT-CT imaging showed distinct tumor labeling using ^{111}In-DOTA-Tz

In addition to tissue harvest biodistribution, we also performed non-invasive SPECT-CT imaging on KPL-4 tumor-bearing mice receiving 7C2, 7C2-TCO$_2$, or 7C2-TCO$_6$ at 5 mg/kg followed 24 hours later by ^{111}In-DOTA-Tz (Figure 5A and B). Mice pre-targeted with non-click reactive 7C2 antibody showed predominantly kidney/bladder uptake at 2 hours with no radioactive signal in circulation or in tumors (Figure 5A), and by 24 hours the small molecule had mostly cleared from the mouse (Figure 5B). Tumors were weakly visualized at 2 hours post ^{111}In-DOTA-Tz injection for both 7C2-TCO$_2$ and 7C2-TCO$_6$ pretargeted groups due in part to high background signal from the blood pool, consistent with systemic click reaction with the proportion of remaining circulating antibody (Figure 5A). However, a portion of excess, non-click reacted tetrazine probe for both 7C2-TCO$_2$ and 7C2-TCO$_6$ groups was evident by enhanced kidney and bladder activity. Using heart as a surrogate for blood pool, the tumor-to-heart ratios derived by image analysis for 7C2-TCO$_2$ and 7C2-TCO$_6$ at 2 hours post ^{111}In-DOTA-Tz were 0.47 and 0.43, respectively, consistent with poor delineation of tumor over background signal.

In contrast, at 24 hours post ^{111}In-DOTA-Tz, SPECT was able to delineate the tumor with much higher tumor-to-heart ratios of 1.40 and 1.40 for 7C2-TCO$_2$ and 7C2-TCO$_6$, respectively, with the higher tumor signal of 7C2-TCO$_6$ being accompanied by higher blood signal (Figure 5B). This suggests that click reaction produced favorable tumor-to-blood ratios after allowing the 7C2-TCO$_x$ click reacted antibodies to further clear systemically and/or accumulate in tumor. Importantly, the amounts of whole body radioactivity of 0.7 MBq for 7C2-TCO$_2$ and 2.1 MBq for 7C2-TCO$_6$ demonstrate the 3-fold improvement in signal due to the corresponding 3-fold difference in click reaction stoichiometry

(Figure 5B). Images from additional mice are available in **Supplemental Figure S5**. Selected mice received ^{111}In-DOTA$_6$-7C2 at 5 mg/kg, as a point of comparison to imaging using traditional (directly) labeled antibodies (Figure 5C). At 28 hours, a substantial amount of tumor uptake had already occurred for ^{111}In-DOTA$_6$-7C2 but was accompanied by significant systemic blood pool activity. At 48 hours, the tumor was well delineated above background, but with almost twice the amount of whole body radioactivity than the 7C2-TCO$_6$ pretargeted group despite receiving a 40% lower injected radioactive dose. Tumor-to heart ratios were consistently higher for traditionally labeled antibody than for pretargeting, with tumor-to-heart ratios of 2.8 and 4.5 for ^{111}In-DOTA$_6$-7C2 at 28 and 48 hours, respectively. In contrast to pretargeted mice, no enhanced bladder or kidney uptake was observed for mice receiving ^{111}In-DOTA$_6$-7C2.

The corresponding pharmacokinetic and tissue distribution data for the SPECT animals (Figure 6) roughly followed a similar trend with the previously acquired tissue harvest data in Figures 3B and 4B. The blood pharmacokinetics of ^{111}In-DOTA-Tz in the absence of click reactive antibody-TCO was comparable to that observed in the non-imaging study (**Supplemental Figure S6**). The amount of ^{111}In-DOTA-Tz present in the blood was relevant to the amount of TCO, with the highest amount present when ^{111}In-DOTA-Tz reacts with 7C2-TCO$_6$ (Figure 6A). The maximum tumor uptake obtained for 7C2-TCO$_6$ followed by ^{111}In-DOTA-Tz was ~6 %ID/g (Figure 6B), which was roughly 3-fold lower than that obtained in the non-imaging, tissue harvest study (Figure 4B). This difference represents a shift in the identity of the limiting reagent for the click reaction, with TCO moiety being the limiting reagent in the SPECT animals, while the ^{111}In-DOTA-Tz was the limiting reagent in the tissue harvest animals (Table 2). The reason for this discrepancy is the requirement of much higher (roughly an order of magnitude) amounts of radioactivity (and
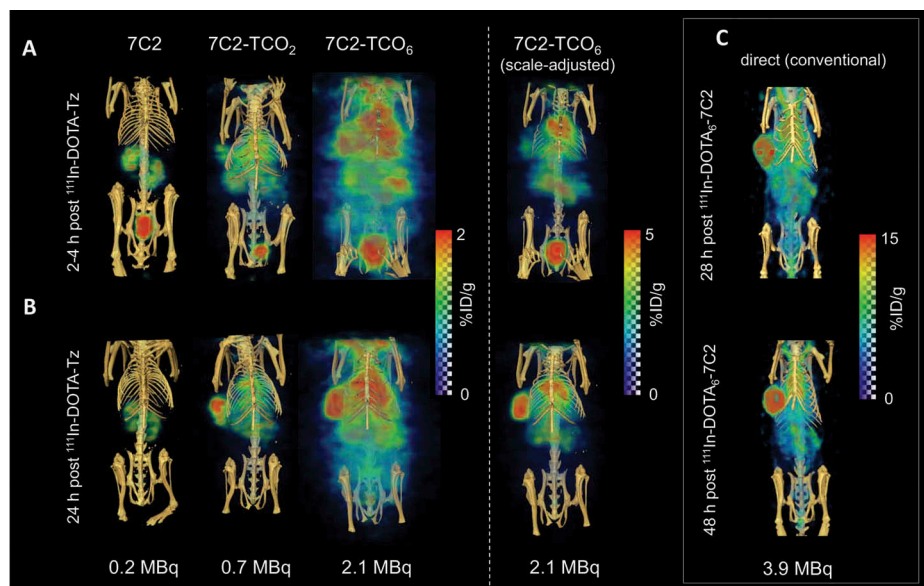

Figure 5. Non-invasive SPECT-CT imaging of *in vivo* click reaction. KPL-4 tumor-bearing mice were injected with 5 mg/kg 7C2 or 7C2-TCO$_x$ antibodies, followed 24 hours later by ^{111}In-labeled tetrazine. Mice were imaged at **(A)** 2-4 hours or **(B)** ~24 hours after injection of ^{111}In-DOTA-Tz (26-28 and 48 hours after injection of antibody, respectively). Amounts of total body radioactivity are indicated under each image at 24 hours post ^{111}In-DOTA-Tz. **(C)** In a separate study, mice received directly labeled ^{111}In-DOTA$_6$-7C2 and were imaged at 28 and 48 hours post injection. Animals from each group were imaged for the same amount of time and images rendered with the same voxel range to indicate relative differences within each group.
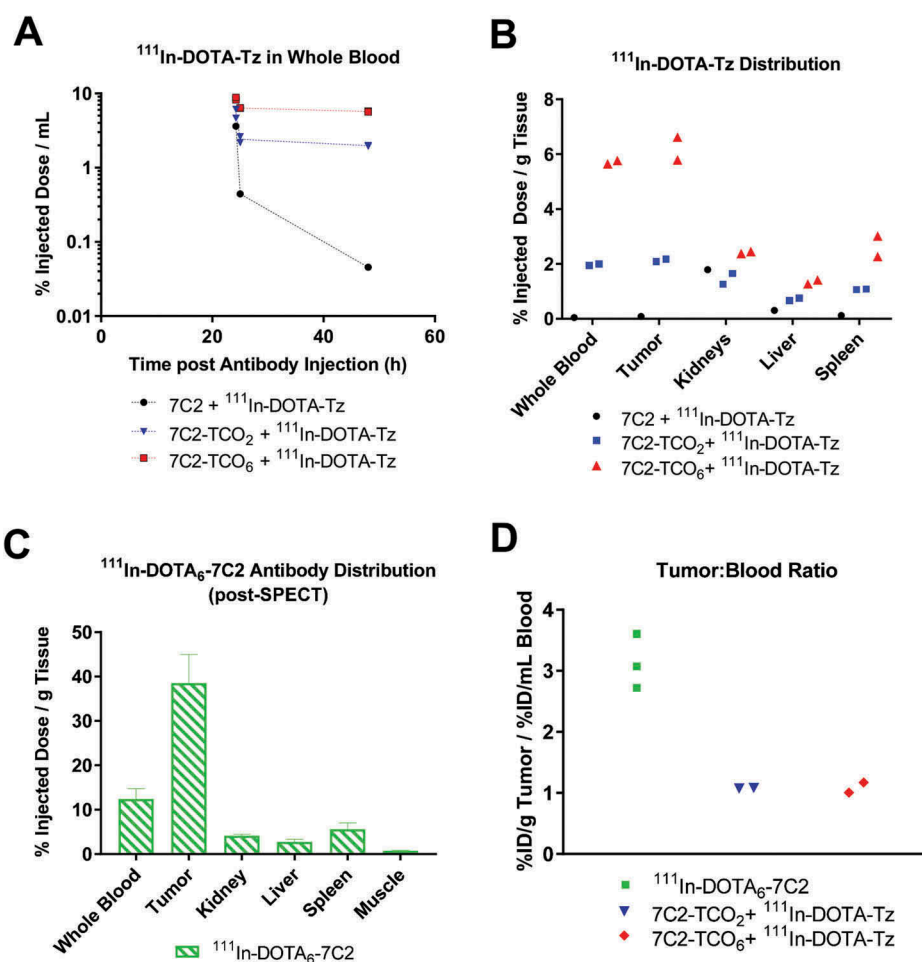
Figure 6. *In vivo* short-term pharmacokinetics and biodistribution of SPECT-CT animals using invasive tissue harvest. KPL-4 tumor-bearing mice received 7C2-TCO$_x$ antibodies (5 mg/kg), followed 24 h later by ^{111}In-DOTA-Tz. Selected control mice received directly labeled ^{111}In-DOTA$_6$-7C2 (5 mg/kg). Whole blood was collected at 24.25, 25 and 48 h post antibody injection followed by 48 h tissue harvest. Both blood and tissue samples were subjected to gamma counting. **(A)** ^{111}In-DOTA-Tz values were plotted as a percentage of injected dose per mL of blood (n<3). **(B)** Percentages of injected dose per gram (%ID/g) for ^{111}In-DOTA-Tz (n<3). **(C)** Distribution of directly labeled ^{111}In-DOTA$_2$-7C2 (n=3). **(D)** ^{111}In signal in tumor normalized to blood.

corresponding increased molar amounts of tetrazine) for SPECT imaging relative to gamma counting, while the dose of TCO-modified antibody was held constant at 5 mg/kg. Tumor uptake for 7C2-TCO$_2$ followed by ^{111}In-DOTA-Tz was ~2 %ID/g, roughly 3-fold lower than the TCO$_6$ variant and perfectly correlating with stoichiometry (Figure 6B). For 7C2, 7C2-TCO$_2$ and 7C2-TCO$_6$, tetrazine uptake was 1.8, 1.5 and 2.4 %ID/g in kidneys and 0.31, 0.71 and 1.3 %ID/g in liver. The tumor uptake for directly labeled ^{111}In-DOTA$_6$-7C2 was almost 40 %ID/g (Figure 6C), comparable to that obtained in the non-imaging arm of the study (Figure 4C). The tumor-to-blood ratio was higher for ^{111}In-DOTA$_6$-7C2 than for 7C2-TCO$_x$ followed by ^{111}In-DOTA-Tz (Figure 6D), where the values obtained by gamma counting (~1) were slightly lower than by image analysis using heart as a surrogate for blood (1.4). Biodistribution data for additional tissues are available in **Supplemental Table S1**.

Discussion

Based on measured whole body radioactivity levels at 48 hours post antibody presented under each image in the lower panel of

Figure 5, the relative radiation exposure is in the following order: 7C2-TCO$_2$ (0.7 MBq) < 7C2-TCO$_6$ (2.1 MBq) < conventional ^{111}In-7C2 (3.9 MBq). However, the conventional (directly labeled) approach produced the highest tumor-to-blood ratio (4.5 relative to 1.4 for both pretargeted groups at a comparable time post antibody (Figure 6)). We believe that 7C2-TCO$_6$ is the preferred pretargeted reagent (despite its similar tumor:blood ratio relative to 7C2-TCO$_2$) due to a greater proportion of the injected radioactivity contributing to image acquisition. However, with same-day imaging being a foremost goal that was not achieved, the conventional approach arguably remains the best among the three options. The tumor signal for 7C2-TCO$_x$ at 2 hours, reflecting the presence of mostly cell-surface HER2 click reaction, is clearly less robust than at 24 hours, when internalization and residualization of radioimmunoconjugates (and catabolites thereof) have occurred. Nevertheless, our pretargeted imaging results are more comparable to conventional imaging than previous efforts with HER2, in which tumor contrast was poor or overshadowed by gut clearance.[20,45] Even if an intermediate imaging time point (e.g., 6 hours) had provided marginal improvements in tumor delineation for 7C2-TCO$_x$,

perhaps in part due to bladder voiding, the persistence of click reaction (radioimmunoconjugate) products in systemic circulation would have likely overshadowed the relatively low same-day tumor signal.

Most literature examples of click-chemistry-based antibody pretargeting have involved non-internalizing targets, many of which were cell-surface glycans such as TAG-72[29–32] and the transmembrane glycoprotein A33.[4,22] Use of a non-internalizing target is conceptually easier because it avoids the complication of receptor turnover, a process that could potentially deplete the available pool of antibody-TCO at the cell surface where click reaction is desirable. Pretargeted imaging with TCO-modified antibodies that internalize is difficult to accomplish with radiolabeled tetrazines like ^{111}In-DOTA-Tz due to their inability to cross cell membranes (owing to the polar/charged nature of the metal-chelate moiety). However, applying the pretargeting approach only to non-internalizing targets greatly limits its utility for imaging applications. The present effort aims to test a pretargeted approach in a clinically relevant model that features an internalizing target.[49] Not only has HER2 been exploited as a signaling target via the therapeutic antibody trastuzumab,[50] it has been further utilized as a drug delivery vector in the antibody-drug conjugate trastuzumab emtansine[51] and in clinical imaging of HER2-positive breast cancer.[40–43] It should be noted, however, that HER2 is a somewhat unusual internalizing oncology target in that it exhibits extremely high expression levels and that trastuzumab binding does not downregulate surface HER2, but instead passively recycles after HER2 endocytosis.[50]

The contrast in pharmacokinetics between the slower clearing, targeting molecule and the rapidly clearing, radioactive molecule plays a key role in achieving a higher signal-to-noise ratio for successful pretargeted imaging. It is therefore critical to establish a well-defined conjugation strategy for antibody modification to ensure that targeting and pharmacokinetics are maintained. The benefits of site-specific radiolabeling techniques for directly labeled imaging agents are well documented.[52] A dendrimer scaffold bearing 8 TCO groups was recently reported; however, it is unclear whether improvements in tumor signal relative to the 2-TCO control were due to differences in stoichiometry, PEG length, presence/absence of dendrimer, or a combination thereof.[53] To allow a more controlled analysis of how stoichiometry affects pretargeted imaging, we used THIOMAB™ antibody conjugation[46] to install TCO moieties via maleimide chemistry site-specifically at 2, 4, or 6 engineered cysteine residues. The importance of site-specific TCO conjugation was evident in our data, as seen by differences in both tumor and blood signal between 7C2-TCO$_2$ and 7C2-TCO$_6$, a comparison that was enabled by recent developments in site-specific conjugation technology.[47] In addition to controlling stoichiometry, this technology also provides pharmacokinetic benefits by avoiding the presence of high antibody conjugation ratio species that, in the case of antibody-drug conjugates, has previously led to increased clearance[54] and may be associated with undesirable biodistribution. Relatively similar antibody binding in vitro suggested that the observed increase in tetrazine signal originated from surface-bound tetrazine (Figure 2). The steady increase in ^{111}In signal with increasing molar TCO ratios indicated an increase in reaction efficiency,

supporting the evaluation of 7C2-TCO$_6$ for in vivo imaging to improve signal-to-noise ratios.

Pretargeting techniques that use a suitably modified (e.g., TCO-conjugated) antibody followed by a radiolabeled small molecule (e.g., radiolabeled tetrazine) could serve as an ideal platform for same-day imaging with less radiation exposure to the patient. We achieved successful imaging using the internalizing target HER2, but with the caveat that much of the click reaction occurred systemically. Although we observed weak tumor visualization as soon as 2 hours after injection of ^{111}In-DOTA-Tz, far superior tumor-to-background contrast was obtained with next-day imaging after the systemically click-reacted antibody had additional time to accumulate at the tumor (Figure 5). We chose a 24-hour time gap between our 7C2-TCO$_x$ and ^{111}In-labeled tetrazine administrations because typical antibody blood concentration does not rapidly decline beyond ~24 hours, which is the approximate end of the pharmacokinetic distribution phase. Nevertheless, a significant amount of systemic (blood) click reaction did occur, suggesting that future efforts to reduce the systemic concentration of mAb-TCO might lead to a more optimal image quality with same-day imaging. This may be achieved through further studies with the use of FcRn mutations or clearing agents.[31,32]

While our 7C2-TCO$_x$ doses were fixed at 5 mg/kg for all studies, the ^{111}In-DOTA-Tz doses were up to 100-fold higher in SPECT-CT animals compared to non-imaging animals (Table 2). This intended discrepancy in study design reflects the fact that higher amounts of radioactivity are needed to acquire SPECT images than for proof-of-concept gamma counting studies. Higher tumor %ID/g values were obtained in non-imaging animals (Figure 4B) because TCO moieties were in excess, and therefore able to react with a greater proportion of administered ^{111}In-DOTA-Tz. In contrast, the ^{111}In-DOTA-Tz in imaging animals was in such vast excess of the available pool of TCO that it over-saturated the system, which resulted in artefactually lower %ID/g values (Figure 6B). In fact, much of the excess injected dose was cleared by renal filtration and subsequently excreted through the urinary bladder as seen in the SPECT-CT images (Figure 5). Evidence for this can also be observed by comparing blood concentrations at 24.25 hours for the 7C2-TCO$_6$ pretargeted group, with non-imaging animals (Figure 3B) having higher blood concentrations of click reacted ^{111}In-DOTA-Tz (21.2%ID/ml) than imaging animals (Figure 6A) (8.5%ID/ml). The lower blood concentration in the latter study demonstrates the limited capacity of circulating TCO for click reaction in imaging mice relative to the higher injected doses of ^{111}In-DOTA-Tz in imaging. The strong correlations between TCO-to-tetrazine ratios (Table 2) and signal in tumor and blood underscore the importance of click reaction stoichiometry.

In summary, we have presented the pretargeted imaging of HER2-expressing tumors by exploiting the click reaction between an ^{111}In-DOTA-Tz and site-specifically TCO-modified anti-HER2 7C2 THIOMAB™ antibodies. In general, both invasive biodistribution and non-invasive SPECT-CT imaging of xenograft-bearing mice showed successful Diel-Alder reaction and subsequent binding and/or internalization of the resulting radioimmunoconjugates. When followed by ^{111}In-DOTA-Tz,

both anti-HER2 7C2 THIOMAB™ antibody variants (having 2 or 6 TCO moieties) provided acceptable SPECT images, with the higher TCO load providing better tumor uptake but also higher blood pool. Our results indicate that click chemistry-based imaging is feasible even with internalizing targets, but that tumor delineation was improved in images obtained one day after the tetrazine probe due to the added benefit of probe internalization and residualization. Most importantly, our work exploits a site-specific conjugation strategy to allow production of precise dienophile-to-mAb ratios such that the importance of IEDDA reaction stoichiometry may be directly assessed.

Materials and methods

Chromatography

Reversed-phase radiochromatography was performed on small molecules injected at 37–74 kBq using an Agilent 1200 HPLC system coupled with a γ-RAM Model 4 radioactive detector (Lab Logic) running Laura version 4 software. A C18 (Phenomenex) column was used at a flow rate of 1 mL/min and a 20-minute gradient of 5% A, 95% B to 95% A, 5% B were utilized, where A = 0.1% trifluoroacetic acid and B = acetonitrile.

Size-exclusion radiochromatography was performed on large molecules injected at 37–74 kBq using an Agilent 1100 HPLC system coupled with a Raytest Gabi Star radioactive flow monitor running ChemStation software. The column was a BioSep SEC S-3000, 300 × 7.8 mm, 5 μm (Phenomenex), with an isocratic phosphate-buffered saline (PBS) mobile phase at 0.5 mL/min for 32 min. The data were collected using ChemStation (3D Systems).

Antibodies

Anti-HER2 THIOMAB™ antibodies (clone 7C2) were engineered with cysteine residues at one or more positions[47] (LC: K149C, LC:K149C+HC:L177C or LC:K149C+HC:L177C+HC: Y376C) for conjugation to the click-reactive linker [(4E)-cyclooct-4-en-1-yl] N-[3-[2-[2-[3-[3-(2,5-dioxopyrrol-1-yl)pro-panoylamino] propoxy]ethoxy]ethoxy]propyl]carbamate (i.e., "TCO-PEG₃-maleimide") to give final conjugates with approximately 2, 4, or 6 TCO groups per antibody, respectively. Conjugation was accomplished by first deblocking the THIOMAB™ antibodies followed by conjugation of TCO-PEG₃-maleimide to the free engineered cysteine residues as previously described.[46] Note that use of PEG spacers for TCO conjugation to mAbs has been evaluated elsewhere.[55] Conjugation of 1,4,7,10-tetraazacyclododecane-1,4,7-tris-acetic acid-10-maleimidoethylacetamide (i.e., "DOTA-maleimide", product #B-272, Macrocyclics, Dallas, TX) to 7C2-LC:K149C and 7C2-LC:K149C+HC:L177C+HC:Y376C (giving DOTA-to-antibody ratio of ~2 and ~6) were also prepared as controls for direct labeling methods used for tissue distribution and imaging, via ^{111}In-DOTA₂-7C2 and ^{111}In-DOTA₆-7C2, respectively.

LC-MS analysis was performed to determine conjugation ratios of immunoconjugates using an Agilent TOF 6530 ESI instrument. Samples were treated with 1:500 w/w Endoproteinase Lys C (Promega, catalog # VA1170) in Tris, pH 7.5, for 30 min at 37°C. The resulting cleavage fragments were loaded onto a 1000 Å, 8 μm PLRP-S (highly cross-linked polystyrene) column heated to 80°C and eluted with a gradient of 30% B to 40% B in 10 minutes. Mobile phase A was H_2O with 0.05% trifluoroacetic acid (TFA) and mobile phase B was acetonitrile with 0.04% TFA. The flow rate was 0.5 ml/min. Protein elution was monitored by UV absorbance detection at 280 nm prior to electrospray ionization and MS analysis. Chromatographic resolution of the unconjugated Fc, residual unconjugated Fab and conjugated Fab was usually achieved. The obtained m/z spectra were deconvoluted using Mass Hunter™ software (Agilent Technologies) to calculate the mass of the antibody fragments.

Tetrazine

DOTA-tetrazine (DOTA-Tz), (Figure 1C) was synthesized by direct conjugation of (4-(1,2,4,5-tetrazin-3-yl)phenyl)metha-namine hydrochloride to 1,4,7,10-tetraazacyclododecane-1,4,7,10-tetraacetic acid mono-N-hydroxysuccinimide ester (i.e., "DOTA-NHS ester", product #B-280, Macrocyclics) as previously reported[56] and purified by reverse-phase chromatography.

Radiochemistry

Free thiols in 7C2 or TCO-7C2 THIOMAB™ antibody conjugates were capped with 2.5 molar equivalents of N-ethyl maleimide and purified by NAP-5 desalting columns (GE Healthcare) prior to iodination to limit potential interference with radioiodination. 7C2, 7C2-TCO₂, 7C2-TCO₄, and 7C2-TCO₆ antibodies were radioiodinated through tyrosine residues by a modified indirect Chizzonite method as previously described.[57] Briefly, ^{125}I was obtained as sodium iodide in 0.1 N sodium hydroxide from Perkin Elmer (Boston, MA). 37 MBq of ^{125}I (~3 μL) was used to label randomly through tyrosine residues at a specific activity of ~370 kBq/μg, with ^{125}I activation achieved using Iodogen tubes (Pierce Chemical Co., Rockford, IL).

Direct radiosynthesis of ^{111}In-DOTAₓ-7C2 was achieved through incubation of ^{111}InCl₃ (Nordion, Ottawa, Canada) with the respective 1,4,7,10-tetraazacyclododecane-1,4,7,10-tetraacetic acid (DOTA)-conjugated molecules in 0.3 M ammonium acetate pH 7 at 37°C for 1 hour as previously described.[57] Purification of all antibody radioimmunoconjugates was achieved using NAP5 columns equilibrated in PBS and confirmed by size-exclusion chromatography.

Radiosynthesis of ^{111}In-DOTA-Tz for invasive biodistribution studies was achieved by incubating 17 μL of DOTA-Tz (0.5 μg/μL) in ammonium acetate buffer, with 37 MBq of ^{111}InCl₃ (in ~3 μL) for 1 hour at 37°C. Radiopurity was assessed using reverse phase HPLC. Production of ^{111}In-DOTA-Tz for SPECT-CT imaging was generated in a larger batch, to accommodate the higher doses needed, at the same radiometal/tetrazine ratio and further purified using 0.1% TFA preconditioned Sep-Pak Plus C18 cartridges (Waters, Milford, MA) using a 50% acetonitrile/water elution, concentrated by rotary evaporation, followed with radiopurity confirmation using reverse phase HPLC.

In vitro KPL-4 click reaction

The HER2-expressing (3+) human breast cancer cell line KPL-4, obtained in 2006 from Dr. J Kurebayashi, was used for both *in vitro* and *in vivo* studies.[58] The cells were cultured in RPMI 1640 media plus 1% L-glutamine with 10% fetal bovine serum. KPL-4 cells were plated at 60,000 cells/well, in 24-well tissue culture plates and allowed to recover for 2 days. Media was replaced with fresh media spiked with iodinated 7C2, 7C2-TCO$_2$, 7C2-TCO$_4$ and 7C2-TCO$_6$ antibodies at 9.25 kBq/well and incubated for 2 h at 37°C. Cells were washed with Hank's Balanced Salt Solution (HBSS) (37°C) three times, followed by addition of fresh media containing ^{111}In-DOTA-Tz at 9.25 kBq/well and incubation for 30 min at 37°C. The short incubation times, 2 hours for antibodies and 30 minutes for tetrazine, were used to minimize antibody internalization and were well below the internalization half-life for HER2 in KPL-4 cells (~12 h).[50] Cells were washed three times with warm HBSS and harvested following incubation with trypsin for 15 min at 37°C. Aliquots of media used for antibody and tetrazine incubation were counted alongside harvested cells using a 2480 Wizard^2 automatic gamma counter (Perkin Elmer). Counts per minute were used to calculate the percent of cell accumulated radiolabeled reagent.

Biodistribution and short-term pharmacokinetics

All animal studies were conducted in accordance with the guidelines of the American Association for Accreditation of Laboratory Animal Care and the Genentech Institutional Animal Care and Use Committee (IACUC). C.B-17 SCID.bg (severe combined immunodeficient; Inbred) female mice (Charles River Laboratories), weighing between 20 to 25 g were inoculated in the right mammary fat pad with ~3 million KPL-4 cells in a 50:50 suspension of HBSS (Invitrogen) and Matrigel (BD Biosciences) in 0.2 mL/mouse. When mean tumor volume reached at least 250 mm^3 mice were randomly assigned into groups. To minimize thyroid sequestration of ^{125}I, 100 μL of 30 mg/mL of sodium iodide was intraperitoneally administered 1 and 24 hours before initial dosing. We performed *in vivo* click reactions using KPL-4 tumor-bearing mice (**Supplemental Figure S1A**). Mice (n = 4 per group) received a single bolus IV injection via the tail vein containing 185 kBq of ^{125}I-7C2, ^{125}I-7C2-TCO$_2$ or ^{125}I-7C2-TCO$_6$ antibodies, at a total dose of 5 mg/kg for each animal. 24 hours later, 185 kBq of ^{111}In-DOTA-Tz was injected via tail vein. A control group received 185 kBq each of ^{125}I-7C2 and ^{111}In-DOTA$_2$-7C2 antibodies, also at a total dose of 5 mg/kg, to serve as a control for traditional (directly labeled) biodistribution methods (**Supplemental Figure S1B**). Blood samples from all mice were collected at 0.25, 24.25, and 72 hours post antibody injection via retroorbital bleed, with terminal tissue harvests performed at 3 days post antibody injection. Terminally collected samples included tumor, kidney, liver, spleen, muscle, fat pad, small intestine, large intestine, lymph nodes, skin, heart, lungs, stomach, brain, and bone marrow. Tissues were collected, rinsed with PBS, weighed and counted for radioactivity using a 2480 Wizard^2 automatic gamma counter (Perkin Elmer). Counts per minute values were used to calculate the percent of injected dose per gram of tissue (%ID/g) as previously described.[57] Error bars represent standard deviation as calculated by GraphPad Prism. For selected figures, significance by Students' t-test is designated by asterisks and/or brackets.

SPECT-CT imaging

Non-invasive *in vivo* distribution was obtained by single photon emission computed tomography/X-ray computed tomography (SPECT-CT) using a modification of previously reported methods.[57] Radiolabeling procedures were identical as for the biodistribution study, except for increased radioactivity amounts and omission of ^{125}I-labeled 7C2 antibodies. Similar to the biodistribution studies, KPL-4 tumor-bearing mice were randomly assigned to groups after the tumors reached at least 250 mm^3. Mice for SPECT imaging received 7C2 (negative control; n = 1), 7C2-TCO$_2$ (n = 2) or 7C2-TCO$_6$ (n = 2) at 5 mg/kg via tail vein injection. A second tail vein injection was administered 24 hours later containing ^{111}In-DOTA-Tz (~18.5 MBq, 1.3 MBq/μg). The TCO-to-tetrazine ratios based on injected doses ranged from 0.025 to 0.075 for 7C2-TCO$_2$ and 7C2-TCO$_6$, respectively (Table 2), suggesting that the injected amount of tetrazine is in excess of available circulating TCO. A control group received ~11 MBq of ^{111}In-DOTA$_6$-7C2 (n = 3) at a total dose of 5 mg/kg. Mice in pretargeting groups were non-invasively imaged at 2–4 h and ~24 h post ^{111}In-labeled tetrazine administration (26–28 and ~48 hours post initial cold antibody injection). Mice in the conventional control group were imaged at 28 and 48 h post ^{111}In-labeled antibody administration. Blood samples for mice in pretargeting groups were collected at 24.25, 25, and 48 hours post antibody injection (0.25, 1, and 24 hours post ^{111}In-labeled tetrazine administration) via retro-orbital bleed, with terminal tissue harvests for all groups (including control) performed at 2 days post antibody injection. Immediately after CT acquisition, SPECT images were acquired in a window centered on two 20% windows centered at the 173- and 247-keV photopeaks of ^{111}In using a high-resolution 5-pinhole collimator and a 5.5 cm radius of rotation. Terminally collected samples were processed as in the invasive biodistribution study. SPECT quantitation was accomplished using Amira software (TGS). Regions of interest were drawn around heart (surrogate for blood exposure) and tumor, based on CT anatomical images.

Abbreviations

%AI	% of Antibody Incubated
%TI	% of Tetrazine Incubated
IEDDA	inverse electron demand Diels-Alder
FcRn	neonatal Fc receptor
mAb	monoclonal antibody
PET	positron emission tomographic
SPECT	single photon emission computed tomographic
TAG-72	tumor-associated glycoprotein 72
TCO	*trans*-cyclooctene
Tz	tetrazine

ORCID

Priya Venkatraman http://orcid.org/0000-0002-6298-3167
Lidia Nazarova http://orcid.org/0000-0001-8010-1167
Gabriel Fung http://orcid.org/0000-0001-5047-3509
Isabel Figueroa http://orcid.org/0000-0001-9204-9132
Cynthia McCaughey http://orcid.org/0000-0002-5049-7399
C. Andrew Boswell http://orcid.org/0000-0002-0426-9846

References

1. Roopenian DC, Akilesh S. FcRn: the neonatal Fc receptor comes of age. Nat Rev Immunol. 2007;7:715–725. doi:10.1038/nri2155.
2. Boswell CA, Brechbiel MW. Development of radioimmunotherapeutic and diagnostic antibodies: an inside-out view. Nucl Med Biol. 2007;34:757–778. doi:10.1016/j.nucmedbio.2007.04.001.
3. Altai M, Membreno R, Cook B, Tolmachev V, Zeglis B. Pretargeted imaging and therapy. J Nucl Med. 2017;58:1553–1559. doi:10.2967/jnumed.117.189944.
4. Zeglis BM, Sevak KK, Reiner T, Mohindra P, Carlin SD, Zanzonico P, Weissleder R, Lewis JS. A pretargeted PET imaging strategy based on bioorthogonal Diels-Alder click chemistry. J Nucl Med. 2013;54:1389–1396. doi:10.2967/jnumed.112.115840.
5. Houghton JL, Membreno R, Abdel-Atti D, Cunanan KM, Carlin S, Scholz WW, Zanzonico PB, Lewis JS, Zeglis BM. Establishment of the in vivo efficacy of pretargeted radioimmunotherapy utilizing inverse electron demand diels-alder click chemistry. Mol Cancer Ther. 2017;16:124–133. doi:10.1158/1535-7163.MCT-16-0503.
6. Bodet-Milin C, Faivre-Chauvet A, Carlier T, Rauscher A, Bourgeois M, Cerato E, et al. Immuno-PET using anticarcinoembryonic antigen bispecific antibody and 68Ga-Labeled peptide in metastatic medullary thyroid carcinoma: clinical optimization of the pretargeting parameters in a first-in-human trial. J Nucl Med. 2016;57:1505–1511. doi:10.2967/jnumed.116.172221.
7. Schuhmacher J, Kaul S, Klivenyi G, Junkermann H, Magener A, Henze M, et al. Immunoscintigraphy with positron emission tomography: gallium-68 chelate imaging of breast cancer pretargeted with bispecific anti-MUC1/anti-Ga chelate antibodies. Cancer Res. 2001;61:3712–3717.
8. Shen S, Forero A, LoBuglio AF, Breitz H, Khazaeli MB, Fisher DR, Wang W, Meredith RF. Patient-specific dosimetry of pretargeted radioimmunotherapy using CC49 fusion protein in patients with gastrointestinal malignancies. J Nucl Med. 2005;46:642–651.
9. Breitz HB, Weiden PL, Beaumier PL, Axworthy DB, Seiler C, Su FM, Graves S, Bryan K, Reno JM. Clinical optimization of pretargeted radioimmunotherapy with antibody-streptavidin conjugate and 90Y-DOTA-biotin. J Nucl Med. 2000;41:131–140.
10. Barbet J, Peltier P, Bardet S, Vuillez JP, Bachelot I, Denet S, Olivier P, Leccia F, Corcuff B, Huglo D, et al. Radioimmunodetection of medullary thyroid carcinoma using indium-111 bivalent hapten and anti-CEA x anti-DTPA-indium bispecific antibody. J Nucl Med. 1998;39:1172–1178.
11. Royzen M, Yap GP, Fox JM. A photochemical synthesis of functionalized trans-cyclooctenes driven by metal complexation. J Am Chem Soc. 2008;130:3760–3761. doi:10.1021/ja8001919.
12. Knall AC, Slugovc C. Inverse electron demand Diels-Alder (iEDDA)-initiated conjugation: a (high) potential click chemistry scheme. Chem Soc Rev. 2013;42:5131–5142. doi:10.1039/c3cs60049a.
13. Thalhammer FW, Wallfahrer U, Sauer J. Reaktivität einfacher offenkettiger und cyclischer dienophile bei Diels–alder-reaktionen mit inversem elektronenbedarf. Tetrahedron Lett. 1990;31:6851–6854. doi:10.1016/S0040-4039(00)97188-0.
14. Blackman ML, Royzen M, Fox JM. Tetrazine ligation: fast bioconjugation based on inverse-electron-demand Diels-Alder reactivity. J Am Chem Soc. 2008;130:13518–13519. doi:10.1021/ja8053805.
15. Selvaraj R, Fox JM. trans-Cyclooctene–a stable, voracious dienophile for bioorthogonal labeling. Curr Opin Chem Biol. 2013;17:753–760. doi:10.1016/j.cbpa.2013.07.031.
16. Denk C, Svatunek D, Mairinger S, Stanek J, Filip T, Matscheko D, Kuntner C, Wanek T, Mikula H. Design, synthesis, and evaluation of a low-molecular-weight 11C-labeled tetrazine for pretargeted PET imaging applying bioorthogonal in vivo click chemistry. Bioconjug Chem. 2016;27:1707–1712. doi:10.1021/acs.bioconjchem.6b00234.
17. Herth MM, Andersen VL, Lehel S, Madsen J, Knudsen GM, Kristensen JL. Development of a 11C-labeled tetrazine for rapid tetrazine-trans-cyclooctene ligation. Chem Commun (Camb). 2013;49:3805–3807. doi:10.1039/c3cc41027g.
18. Denk C, Svatunek D, Filip T, Wanek T, Lumpi D, Frohlich J, Kuntner C, Mikula H. Development of a 18F-labeled tetrazine with favorable pharmacokinetics for bioorthogonal PET imaging. Angew Chem Int Ed Engl. 2014;53:9655–9659. doi:10.1002/anie.201404277.
19. Devaraj NK, Thurber GM, Keliher EJ, Marinelli B, Weissleder R. Reactive polymer enables efficient in vivo bioorthogonal chemistry. Proc Natl Acad Sci USA. 2012;109:4762–4767. doi:10.1073/pnas.1113466109.
20. Keinanen O, Fung K, Pourat J, Jallinoja V, Vivier D, Pillarsetty NK, Airaksinen AJ, Lewis JS, Zeglis BM, Sarparanta M. Pretargeting of internalizing trastuzumab and cetuximab with a 18F-tetrazine tracer in xenograft models. EJNMMI Res. 2017;7:95. doi:10.1186/s13550-017-0344-6.
21. Cook BE, Adumeau P, Membreno R, Carnazza KE, Brand C, Reiner T, Agnew BJ, Lewis JS, Zeglis BM. Pretargeted PET imaging using a site-specifically labeled immunoconjugate. Bioconjug Chem. 2016;27:1789–1795. doi:10.1021/acs.bioconjchem.6b00235.
22. Zeglis BM, Brand C, Abdel-Atti D, Carnazza KE, Cook BE, Carlin S, Reiner T, Lewis JS. Optimization of a pretargeted strategy for the PET imaging of colorectal carcinoma via the modulation of radioligand pharmacokinetics. Mol Pharm. 2015;12:3575–3587. doi:10.1021/acs.molpharmaceut.5b00294.
23. Houghton JL, Zeglis BM, Abdel-Atti D, Sawada R, Scholz WW, Lewis JS. Pretargeted Immuno-PET of pancreatic cancer: overcoming circulating antigen and internalized antibody to reduce radiation doses. J Nucl Med. 2016;57:453–459. doi:10.2967/jnumed.115.163824.
24. Adumeau P, Carnazza KE, Brand C, Carlin SD, Reiner T, Agnew BJ, Lewis JS, Zeglis BM. A pretargeted approach for the multimodal PET/NIRF imaging of colorectal cancer. Theranostics. 2016;6:2267–2277. doi:10.7150/thno.16744.
25. Garcia MF, Zhang X, Shah M, Newton-Northup J, Cabral P, Cerecetto H, Quinn T. 99mTc-bioorthogonal click chemistry reagent for in vivo pretargeted imaging. Bioorg Med Chem. 2016;24:1209–1215. doi:10.1016/j.bmc.2016.01.046.
26. Yazdani A, Janzen N, Czorny S, Ungard RG, Miladinovic T, Singh G, Valliant JF. Preparation of tetrazine-containing [2 + 1] complexes of 99mTc and in vivo targeting using bioorthogonal inverse electron demand Diels-Alder chemistry. Dalton trans. 2017;46:14691–14699. doi:10.1039/c7dt01497j.
27. Yazdani A, Bilton H, Vito A, Genady AR, Rathmann SM, Ahmad Z, Janzen N, Czorny S, Zeglis BM, Francesconi LC, et al. A bone-seeking trans-cyclooctene for pretargeting and bioorthogonal chemistry: a

proof of concept study using ^{99}mTc- and ^{177}Lu-Labeled tetrazines. J Med Chem. 2016;59:9381–9389. doi:10.1021/acs.jmedchem.6b00938.

28. Altai M, Perols A, Tsourma M, Mitran B, Honarvar H, Robillard M, Rossin R, Ten Hoeve W, Lubberink M, Orlova A, et al. Feasibility of affibody-based bioorthogonal chemistry-mediated radionuclide pretargeting. J Nucl Med. 2016;57:431–436. doi:10.2967/jnumed.115.162248.

29. Rossin R, van den Bosch SM, Ten Hoeve W, Carvelli M, Versteegen RM, Lub J, Robillard MS. Highly reactive trans-cyclooctene tags with improved stability for Diels-Alder chemistry in living systems. Bioconjug Chem. 2013;24:1210–1217. doi:10.1021/bc400153y.

30. Rossin R, Verkerk PR, van den Bosch SM, Vulders RC, Verel I, Lub J, Robillard MS. In vivo chemistry for pretargeted tumor imaging in live mice. Angew Chem Int Ed Engl. 2010;49:3375–3378. doi:10.1002/anie.200906294.

31. Rossin R, Lappchen T, van den Bosch SM, Laforest R, Robillard MS. Diels-Alder reaction for tumor pretargeting: in vivo chemistry can boost tumor radiation dose compared with directly labeled antibody. J Nucl Med. 2013;54:1989–1995. doi:10.2967/jnumed.113.123745.

32. Rossin R, van Duijnhoven SM, Lappchen T, van den Bosch SM, Robillard MS. Trans-cyclooctene tag with improved properties for tumor pretargeting with the diels-alder reaction. Mol Pharm. 2014;11:3090–3096. doi:10.1021/mp500275a.

33. Lappchen T, Rossin R, van Mourik TR, Gruntz G, Hoeben FJM, Versteegen RM, Janssen HM, Lub J, Robillard MS. DOTA-tetrazine probes with modified linkers for tumor pretargeting. Nucl Med Biol. 2017;55:19–26. doi:10.1016/j.nucmedbio.2017.09.001.

34. Oliveira BL, Guo Z, Bernardes GJL. Inverse electron demand Diels-Alder reactions in chemical biology. Chem Soc Rev. 2017;46:4895–4950. doi:10.1039/c7cs00184c.

35. Wu H, Devaraj NK. Inverse electron-demand diels-alder bioorthogonal reactions. Top Curr Chem (Cham). 2016;374:3. doi:10.1007/s41061-015-0005-z.

36. Meyer JP, Adumeau P, Lewis JS, Zeglis BM. Click chemistry and radiochemistry: the first 10 years. Bioconjug Chem. 2016;27:2791–2807. doi:10.1021/acs.bioconjchem.6b00561.

37. Patra M, Zarschler K, Pietzsch HJ, Stephan H, Gasser G. New insights into the pretargeting approach to image and treat tumours. Chem Soc Rev. 2016;45:6415–6431. doi:10.1039/c5cs00784d.

38. Shi X, Gao K, Huang H, Gao R. Pretargeted Immuno-PET based on bioorthogonal chemistry for imaging EGFR positive colorectal cancer. Bioconjug Chem. 2018;29:250–254. doi:10.1021/acs.bioconjchem.8b00023.

39. Billaud EMF, Belderbos S, Cleeren F, Maes W, van de Wouwer M, Koole M, Verbruggen A, Himmelreich U, Geukens N, Bormans G. Pretargeted PET imaging using a bioorthogonal ^{18}F-Labeled trans-cyclooctene in an ovarian carcinoma model. Bioconjug Chem. 2017;28:2915–2920. doi:10.1021/acs.bioconjchem.7b00635.

40. Dijkers EC, Oude Munnink TH, Kosterink JG, Brouwers AH, Jager PL, de Jong JR, van Dongen GA, Schröder CP, Lub-de Hooge MN, de Vries EG. Biodistribution of ^{89}Zr-trastuzumab and PET imaging of HER2-positive lesions in patients with metastatic breast cancer. Clin Pharmacol Ther. 2010;87:586–592. doi:10.1038/clpt.2010.12.

41. Ulaner GA, Lyashchenko SK, Riedl C, Ruan S, Zanzonico PB, Lake D, et al. 2018. First-in-human her2-targeted imaging using (89)zr-pertuzumab pet/ct: dosimetry and clinical application in patients with breast cancer. J Nucl Med. 2018;59:900–906. doi:10.2967/jnumed.117.202010.

42. Holloway CM, Scollard DA, Caldwell CB, Ehrlich L, Kahn HJ, Reilly RM. Phase I trial of intraoperative detection of tumor margins in patients with HER2-positive carcinoma of the breast following administration of ^{111}In-DTPA-trastuzumab Fab fragments. Nucl Med Biol. 2013;40:630–637. doi:10.1016/j.nucmedbio.2013.03.005.

43. Sandstrom M, Lindskog K, Velikyan I, Wennborg A, Feldwisch J, Sandberg D, Tolmachev V, Orlova A, Sörensen J, Carlsson J, et al. Biodistribution and radiation dosimetry of the Anti-HER2 affibody molecule ^{68}Ga-ABY-025 in breast cancer patients. J Nucl Med. 2016;57:867–871. doi:10.2967/jnumed.115.169342.

44. Pereira PMR, Abma L, Henry KE, Lewis JS. Imaging of human epidermal growth factor receptors for patient selection and response monitoring - From PET imaging and beyond. Cancer Lett. 2018;419:139–151. doi:10.1016/j.canlet.2018.01.052.

45. Knight JC, Mosley M, Uyeda HT, Cong M, Fan F, Faulkner S, Cornelissen B. In vivo pretargeted imaging of HER2 and TAG-72 expression using the HaloTag Enzyme. Mol Pharm. 2017;14:2307–2313. doi:10.1021/acs.molpharmaceut.7b00172.

46. Junutula JR, Raab H, Clark S, Bhakta S, Leipold DD, Weir S, et al. Site-specific conjugation of a cytotoxic drug to an antibody improves the therapeutic index. Nat Biotechnol. 2008;26:925–932. doi:10.1038/nbt.1480.

47. Ohri R, Bhakta S, Fourie-O'Donohue A, Dela Cruz-Chuh J, Tsai SP, Cook R, et al. High-throughput cysteine scanning to identify stable antibody conjugation sites for maleimide- and disulfide-based linkers. Bioconjug Chem. 2018. doi:10.1021/acs.bioconjchem.7b00791.

48. Pastuskovas CV, Mundo EE, Williams SP, Nayak TK, Ho J, Ulufatu S, et al. Effects of anti-VEGF on pharmacokinetics, biodistribution, and tumor penetration of trastuzumab in a preclinical breast cancer model. Mol Cancer Ther. 2012;11:752–762. doi:10.1158/1535-7163.MCT-11-0742-T.

49. Rudnick SI, Lou J, Shaller CC, Tang Y, Klein-Szanto AJ, Weiner LM, Marks JD, Adams GP. Influence of affinity and antigen internalization on the uptake and penetration of Anti-HER2 antibodies in solid tumors. Cancer Res. 2011;71:2250–2259. doi:10.1158/0008-5472.CAN-10-2277.

50. Austin CD, de Maziere AM, Pisacane PI, van Dijk SM, Eigenbrot C, Sliwkowski MX, Klumperman J, Scheller RH. Endocytosis and sorting of ErbB2 and the site of action of cancer therapeutics trastuzumab and geldanamycin. Mol Biol Cell. 2004;15:5268–5282. doi:10.1091/mbc.e04-07-0591.

51. Junutula JR, Flagella KM, Graham RA, Parsons KL, Ha E, Raab H, et al. Engineered thio-trastuzumab-DM1 conjugate with an improved therapeutic index to target human epidermal growth factor receptor 2-positive breast cancer. Clin Cancer Res. 2010;16:4769–4778. doi:10.1158/1078-0432.CCR-10-0987.

52. Adumeau P, Sharma SK, Brent C, Zeglis BM. Site-specifically labeled immunoconjugates for molecular imaging–part 1: cysteine residues and glycans. Mol Imaging Biol. 2016;18:1–17. doi:10.1007/s11307-015-0919-4.

53. Cook BE, Membreno R, Zeglis BM. Dendrimer scaffold for the amplification of in vivo pretargeting ligations. Bioconjug Chem. 2018;29:2734–2740. doi:10.1021/acs.bioconjchem.8b00385.

54. Hamblett KJ, Senter PD, Chace DF, Sun MM, Lenox J, Cerveny CG, et al. Effects of drug loading on the antitumor activity of a monoclonal antibody drug conjugate. Clin Cancer Res. 2004;10:7063–7070. doi:10.1158/1078-0432.CCR-04-0789.

55. Rondon A, Ty N, Bequignat JB, Quintana M, Briat A, Witkowski T, et al. Antibody PEGylation in bioorthogonal pretargeting with trans-cyclooctene/tetrazine cycloaddition: in vitro and in vivo evaluation in colorectal cancer models. Sci Rep. 2017;7:14918. doi:10.1038/s41598-017-15051-y.

56. Zeglis BM, Mohindra P, Weissmann GI, Divilov V, Hilderbrand SA, Weissleder R, Lewis JS. Modular strategy for the construction of radiometalated antibodies for positron emission tomography based on inverse electron demand Diels-Alder click chemistry. Bioconjug Chem. 2011;22:2048–2059. doi:10.1021/bc200288d.

57. Mandikian D, Takahashi N, Lo AA, Li J, Eastham-Anderson J, Slaga D, et al. Relative target affinities of T cell-dependent bispecific antibodies determine biodistribution in a solid tumor mouse model. Mol Cancer Ther. 2018;17:776–785. doi:10.1158/1535-7163.MCT-17-0657.

58. Kurebayashi J, Otsuki T, Tang CK, Kurosumi M, Yamamoto S, Tanaka K, Mochizuki M, Nakamura H, Sonoo H. Isolation and characterization of a new human breast cancer cell line, KPL-4, expressing the Erb B family receptors and interleukin-6. Br J Cancer. 1999;79:707–717. doi:10.1038/sj.bjc.6690114.